



## **Latest SCC Issues of Core Shroud and Recirculation Piping in Japanese BWRs**

Yuichi Okamura, Akihiro Sakashita, Toshihiko Fukuda, Hironobu Yamashita and Tsuneo Futami

Tokyo Electric Power Co. (TEPCO), Japan

### **ABSTRACT**

This paper reports that a high incidence of stress corrosion cracking (SCC) cracks have been found in the core Shroud and PLR piping of several Japanese BWR plants. The results of investigations show the cracks to be of SCC type in 316L stainless steel and with different characteristics from the type in 304 stainless steel. The cracks on the shroud surface were mainly verified near the shroud ring weld line and core region weld line, and the crack shape could be classified into two types: one type was circumferential cracking in the shroud ring, and the other was isolated occurrences of radial cracking in the core region. The structural integrity of those shrouds with cracks was evaluated under a conservative assumption and confirmed to be adequate. A relatively large error was identified in measuring the crack depth in the PLR piping.

**KEY WORDS:** BWR, SCC, IGSCC, TGSCC, shroud, PLR piping, low carbon stainless steel, 316L, stress, crack, crack growth rate, stress intensity factor, harden layer, ferrite, UT accuracy, structural integrity

### **1. INTRODUCTION**

As of May 2003, many Japanese plants have been stopped for inspection and repair work because of SCC occurrences. Such cracks have been found in the core shroud and primary recirculation piping fabricated from low carbon stainless steel such as type 316L which contains less than 0.02% carbon and is believed to be resistant to SCC. This paper reports the latest status of inspection, investigation and structural evaluation of SCC occurrences in Japanese BWR plants.

#### **1.1 Chronology of SCC Issue in Japanese BWRs**

Stress corrosion cracking (SCC) frequently occurred in Japanese BWR plants in the heat-affected zone of the welds in PLR piping fabricated from type 304 SS during the late 1970s, similarly to the occurrences in overseas plants. As a corrective measure for this problem, utilities and plant manufacturers have jointly developed since 1977 type 316L SS that is excellent in property for anti-sensitization, and Nuclear Power Engineering Center (NUPEC) as a government authority has demonstrated the reliability of type 316L. This material was used for the PLR piping of TEPCO Fukushima-Daini unit No. 2 (2F-2), which started commercial operation in February 1984, and has become the standard specification for PLR piping material. The adoption of low-carbon SS was considered to be the only solution to SCC in those days. Similar SCC occurrences were found on the shroud upper ring fabricated from type 304 SS in Fukushima-Daiichi unit No. 2 (1F-2) in 1994. The shrouds made from type 304 SS, including those in 1F-2, have all been replaced with those made from type 316L SS during the period from 1997 to 2001.

Although SCC on the pressure vessel nozzle safe end made of type 316L SS in U.S. Peach Bottom 2 was reported in 1985, this was regarded as a phenomenon peculiar to this particular plant. However, plant manufacturers have been studying SCC in low-carbon SS since 1992, and presented a relationship between the hardness of the material and its sensitivity to SCC cracking for type 316L at a conference of the American Nuclear Society in 1995. Ultrasonic inspection of PLR piping was conducted during the periodic inspection of Chubu Electric Power Co. Hamaoka-3 plant in 1995, when a UT echo from the inner surface was accepted as evidence for the existence of a crack. In the following year, a sample of the piping was sectioned and a detailed inspection was performed. Several longitudinal cracks were discovered near the welding line. Since there was no sensitization in the material, it was considered that the possibility of a manufacturing defect such as high-temperature cracking during the heat treatment was more likely than that of SCC.

During 1994 and since, SCC occurrences in type 304L SS have been reported from overseas. More recently, cracking was identified in the reactor core shroud lower ring (H6a welding line) made from 316L SS in Fukushima-Daini unit No. 3 plant (2F-3) in July 2001. A hardened layer on the surface exceeding Hv300 was verified, and it

became clear that transgranular SCC (TGSCC) had occurred from this hardened layer. Repair with tie rods was carried out. Subsequently, in the periodic inspection starting in August 2002 of Kashiwazaki-Kariwa unit No. 3 (KK-3), cracks were identified on the inner side of the shroud support ring (H7a welding line) and outside of the shroud lower ring (H6a welding line). Moreover, cracks have also been found near the welding line in PLR piping fabricated from type 316L SS in several domestic BWR plants.

## 2. SCC ON CORE SHROUD

### 2.1 Results of Inspection

An inspection was performed on the core shroud in nine domestic plants by a remote-controlled underwater camera, which can discriminate a 1mil wire, and ultrasonic equipment. The cracking shown in Table 1 was found as a result of this inspection. Circumferential cracks in the shroud were verified on the inner surface of the shroud support ring (H7a welding line) and on the outer surface of the lower ring (H6a welding line). Isolated occurrences of radial cracking were also observed near the core region (H4 welding line). The size of these isolated radial cracks was about 10 mm in both width and height, and one of 180mm in width was also found in 1F-4.

Table 1. Status of SCC on Shroud (as of May 2003)

Plant	Weld line / Surface side	Location	Shape	Number of cracks	Crack length (mm)
Onagawa 1	H2 / outer	Ring	straight	Circumferential many	10
	H6a / outer	Ring	straight	Circumferential many	-
1F-4	H4 / inner	Shell	radial	1	H80,W180
2F-2	H3 / inner	Ring	straight	2	30
	H3 / inner	Shell	radial	5	H30,W25
	H3 / outer	Weld metal	radial	3	H17,W40
	H4 / inner	Shell	straight and/or radial	17	H30,W200
	H4 / inner	Shell	radial	7	H90,W80
2F-3	H3 / inner	Ring	straight	1	8
	H3 / inner	Ring	straight	10	210
	H3 / inner	Shell	straight	1	13
	H4 / inner	Shell	radial	1	H30,W16
2F-4	H3 / inner	Shell	straight	5	30
	H4 / inner	Shell	radial	1	H19,W31
	H4 / outer	Shell	radial	1	H15,W11
KK-1	H3 / inner	Ring	straight	9	145
	H4 / inner	Shell	radial	1	H22,W32
	H4 / outer	Shell	radial	3	H20,W10
KK-2	H1 / outer	Ring	straight	1	90
	H6a / outer	Ring	straight	Circumferential many	-
	V16 / outer	Shell	radial	1	20
	H7 / outer	Ring	straight	Circumferential many	-
KK-3	H6a / outer	Ring	straight	Circumferential many	-
	H7a / inner	Ring	straight	Circumferential many	-
Hamaoka 4	H6a / outer	Ring	straight	Circumferential many	-

### 2.2 Investigations of Core Shroud Cracking

Results of a detailed investigation on boat samples from a cracked shroud are shown in Figure 3. SEM observations indicate the mechanism common to low-carbon stainless steel SCC of the initiation of cracking occurring in a hardened layer of the surface as TGSCC, and TGSCC subsequently changing into IGSCC. The sample of H7a from KK-3 shows that a deteriorated layer whose hardness exceeds Hv300 was formed on a finish-machined surface such as a shroud ring

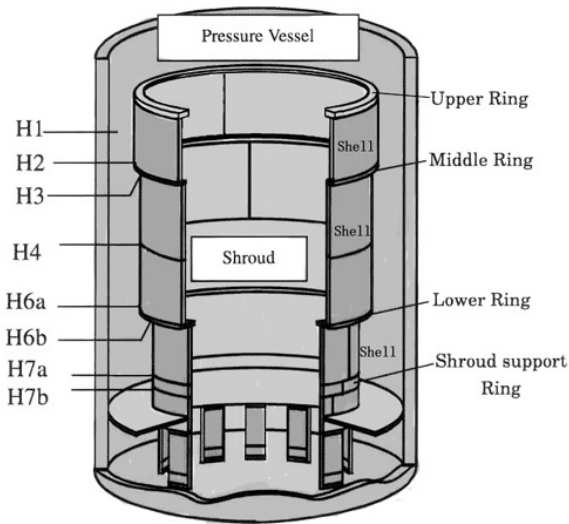


Fig. 1. Shroud weld lines

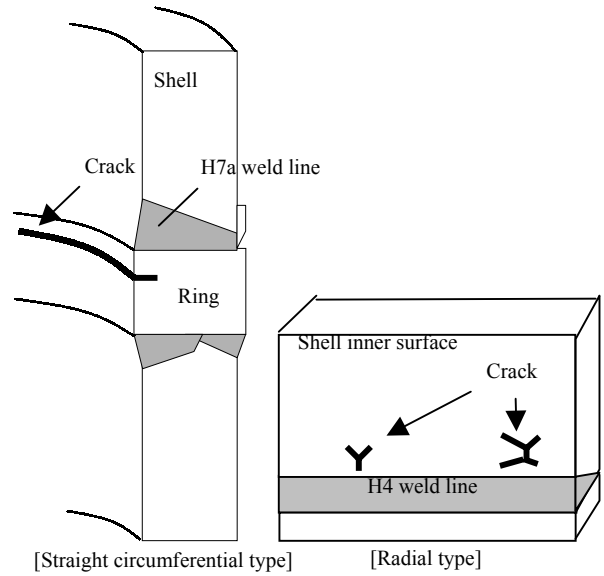


Fig. 2. Typical crack shape pattern

during the manufacturing process, the thickness of this layer being about  $100\ \mu\text{m}$ . The sample of H4 from KK-1, a case of a ground-finished surface such as the cylindrical core region, showed a very thin hardened layer of about  $30\ \mu\text{m}$  in thickness. The results of a chemical composition analysis of the sample showed no obvious sensitization near the welding line such as a concentration of chromium at the grain boundary. Most of the crack shapes such as the isolated radial ones were proved to depend on the local residual stress distribution on the surface.

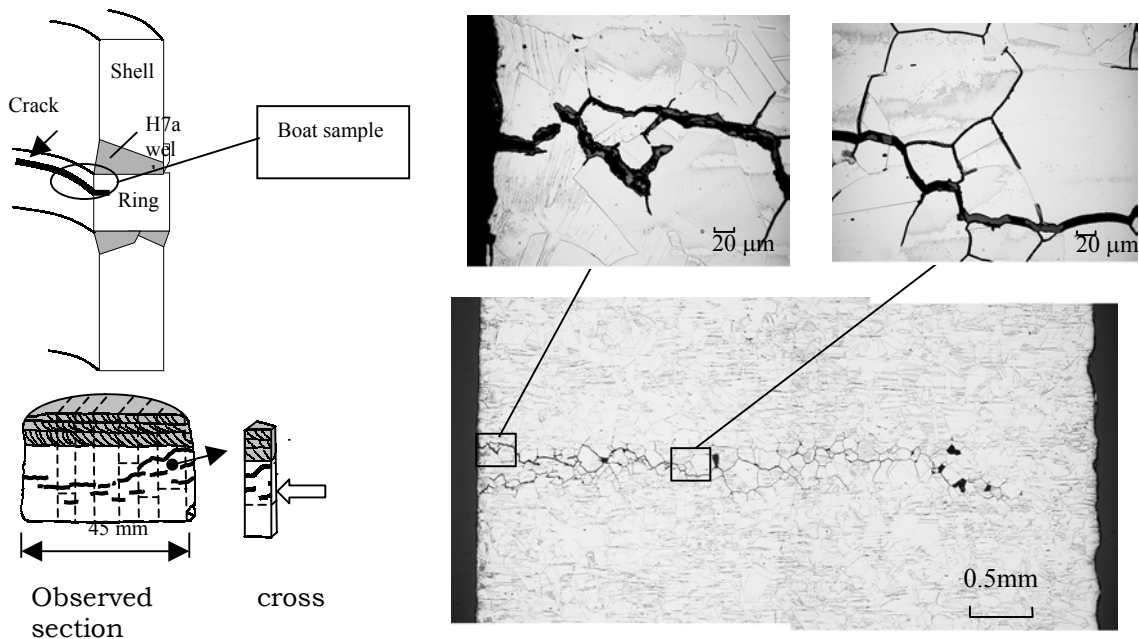


Fig. 3. SEM observations of typical SCC crack (KK-3 shroud H7a)

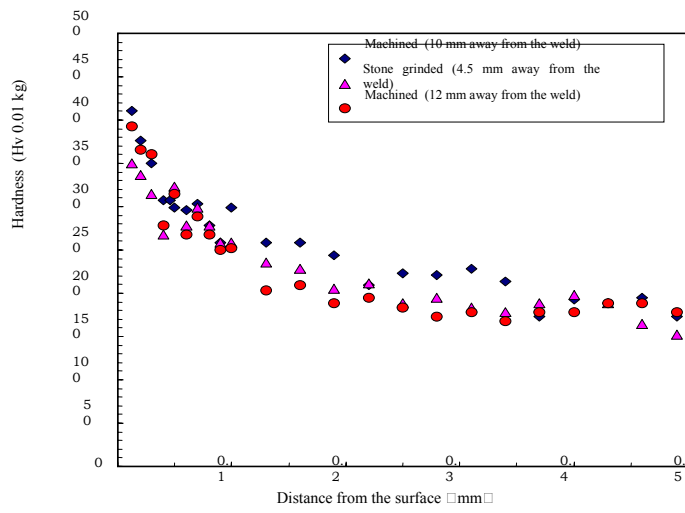


Fig. 4. Distributions of hardness with depth (KK-3 shroud H7a )

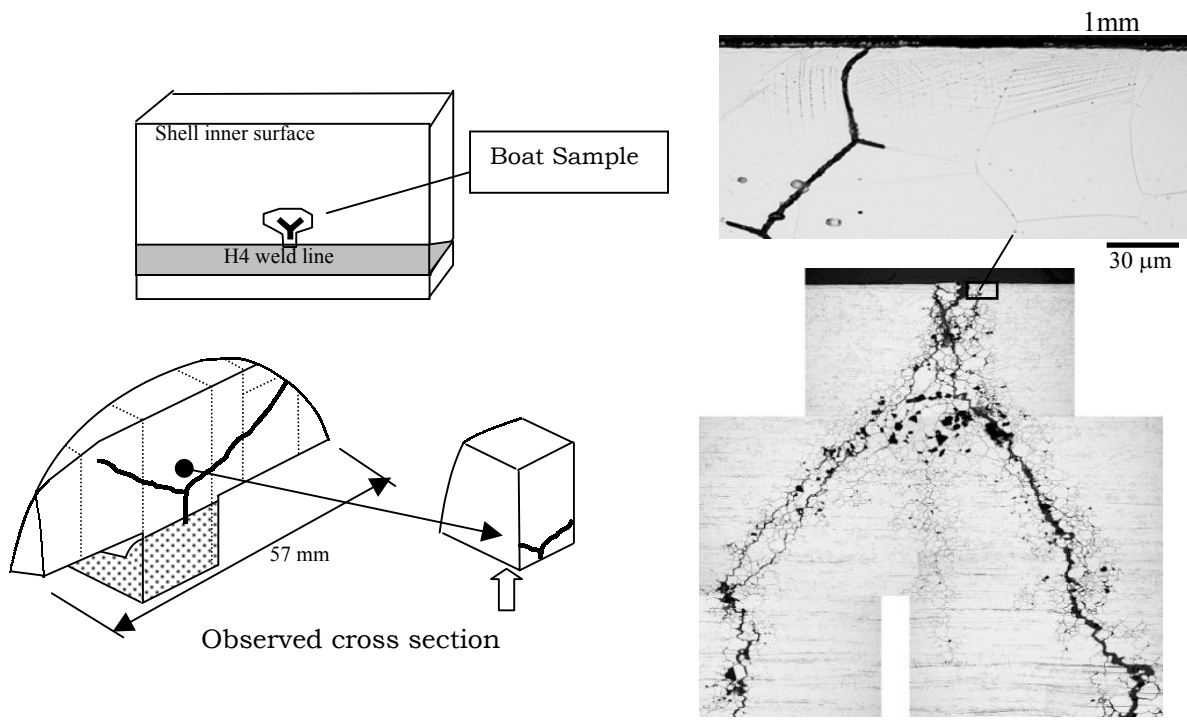


Fig. 5. SEM observation of SCC crack (KK-1 shroud H4)

### 3. SCC IN PLR PIPING

#### 3.1 Results of Inspection

Many cracks in PLR piping were found during March 2003 in several plants as shown in Table 2. The welds in the PLR piping were inspected by an ultrasonic test from the external surface. Cracks were found near the welds inside the piping. This cracking was distributed throughout the whole of the recirculation piping (see Fig. 6) and there was no specific pattern

Table 2. SCC in PLR pipings of Japanese BWRs (as of May 2003)

Plant	System A or B	Total number of weld lines	Number of cracked weld lines	Crack shape	Crack length (mm: min - max)	Crack depth (mm: min - max) [ ]: UT / sampling
Onagawa 1	A	32	3	straight	10 - 43	O.D. - 4.0 [0 / 6.1]
	B	34	7	straight	4 - 172	O.D. - 5.5 [3 / 12.2]
2F-2	A	41	1	straight	2 - 6	3 - 4.8
	B	44	(Inspecting)	(Inspecting)	(Inspecting)	(Inspecting)
2F-3	A	31	3	straight	5 - 50	1 - 5.5 [3.5 / 6.7]
	B	32	8	straight	3 - 287	1.5 - 7 [4 / 6.3]
2F-4	A	33	1	straight	2 - 14	O.D. - 4.4 [4.4 / 5.8]
	B	35	2	straight	2 - 121	3.3 - 7.8
K-1	A	37	15	straight	Spot - 50	O.D. - 7.0 [4.5 / 7.3]
	B	35	16	straight	Spot- 141	O.D. - 6.0
K-2	A	33	1	straight	O.D.	2.1
	B	33	2	straight	Spot - 10	O.D. - 3.5
K-3	A	31	2	straight	O.D. - 35	2 - 6.5
Hamaoka 1	A	32	1	straight	9 - 30	O.D.
	B	33	1	straight	22	O.D.
Hamaoka 3	A	31	4	straight	O.D. - 33	O.D. - 4.3 [2.8 / 5.5]
	B	31	3	straight	6 - 15	1.7 - 4.3 [3.5 / 6.5]
Hamaoka 4	A	29	2	straight	4 - 13	O.D.

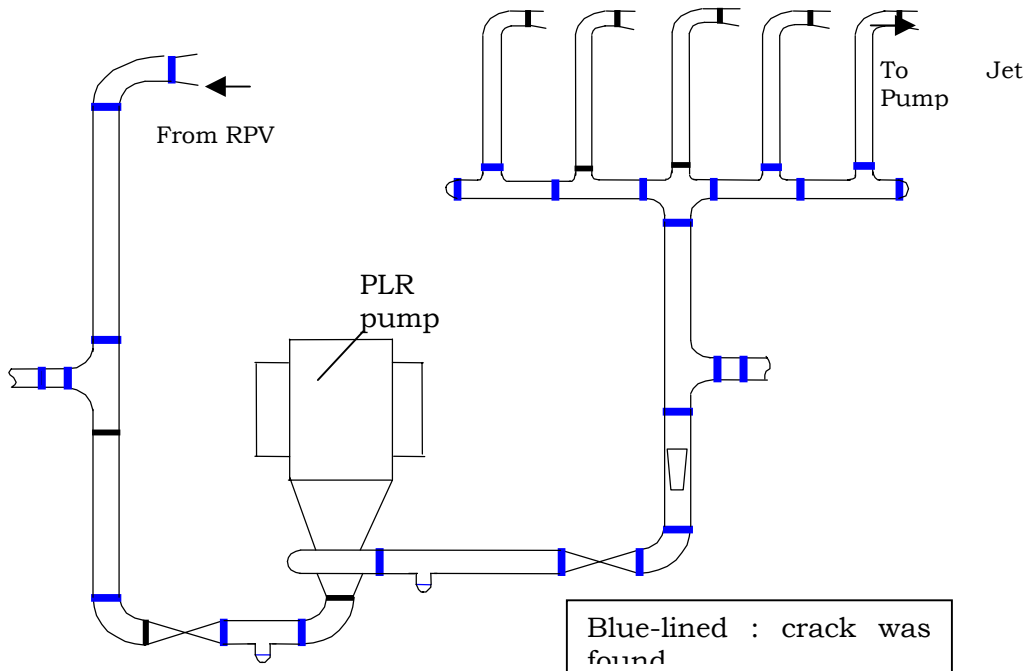


Fig. 6. Map of weld Cracking in primary recirculation piping (cumulative)

### 3.2 Observation of PLR Piping Samples

Samples of PLR piping welds were taken from KK-1. The thickness of the hardened layer was found to be 20  $\mu\text{m}$  on the inner surface of the PLR piping. We elucidated that TGSCC had been initiated from this surface layer and propagated to the inside of the pipe material by IGSCC. In some cases, the crack had penetrated the welding metal itself. The deteriorated layer whose hardness exceeded Hv300 was also formed on the inner surface of the pipe joints that had been machine-finished during the manufacturing process. It was found that the amount of ferrite had decreased to 5% or less in the boundary part of the weld metal due to the dilution of ferrite between the pipe materials, which hardly included any ferrite, and the weld metal, which contained a large amount of ferrite. This resulted in the shortage of ferrite in the weld metal. Measured data for a sample of welded PLR pipe are shown in Figure 9. No obvious sensitization at the grain boundaries was apparent, and the shape of most of the cracks also depended on the local residual stress distribution on the surface.

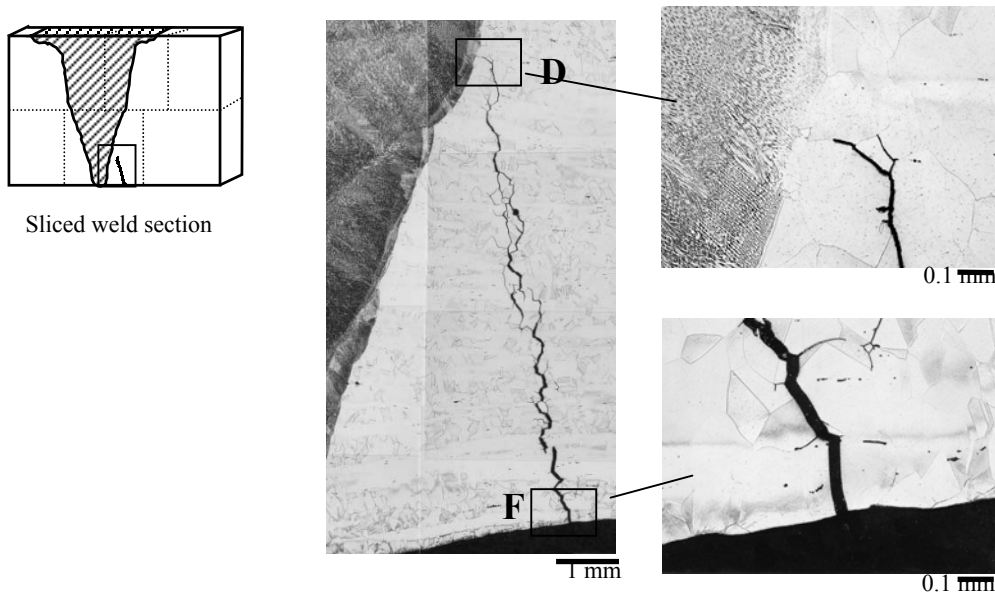


Fig. 7. SEM observation of cracks in welded PLR piping (KK-1)

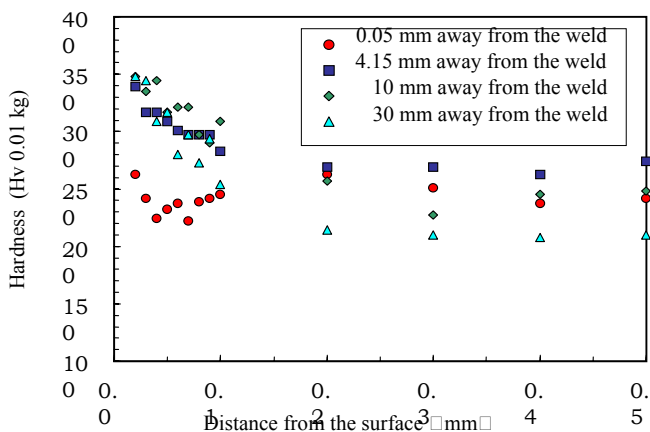


Fig. 8. Hardness Distributions with depth (KK-1)

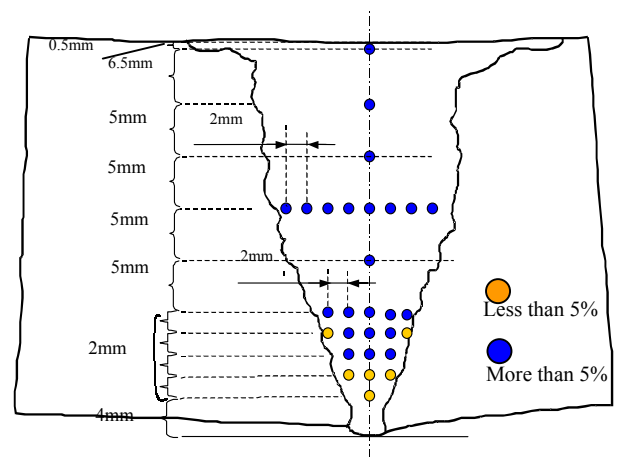


Fig. 9. Ferrite percentage in the weld metal of PLR piping (Onagawa-1)

### 3.3 Discussion on the Accuracy of Crack Depth Measurement of PLR Piping

An ultrasonic inspection was carried out on PLR piping. The creeping wave method, which is hardly influenced by the signal reflected from the back surface, was applied for measuring the crack length in the circumferential direction, and the accuracy of the method was deemed to be appropriate. However, for measuring the crack depth, the share wave crack tip echo method was applied, and a substantial difference was apparent between the actual depth and that estimated from UT data. The reason for this error being generated in crack depth measurements was the direction of crack propagation toward the weld metal. When the crack propagates into the weld metal, the signal strength is significantly reduced and the echo from the crack tip cannot return to the surface. In such a case, a longitudinal ultrasonic wave is known to be more effective in the weld metal. Satisfactory results can be expected with longitudinal wave UT and phased array UT for field inspection in actual plants. It is planned to extract actual plant data further and check the validity of these measurement methods from now on. Since this problem with the accuracy of crack measurement by UT arose, evaluation of the integrity by using the present UT data has been concluded to be uncertain. It was therefore decided that the cracks needed to be removed or the piping locally replaced until sufficient accuracy of crack measurement could be established.

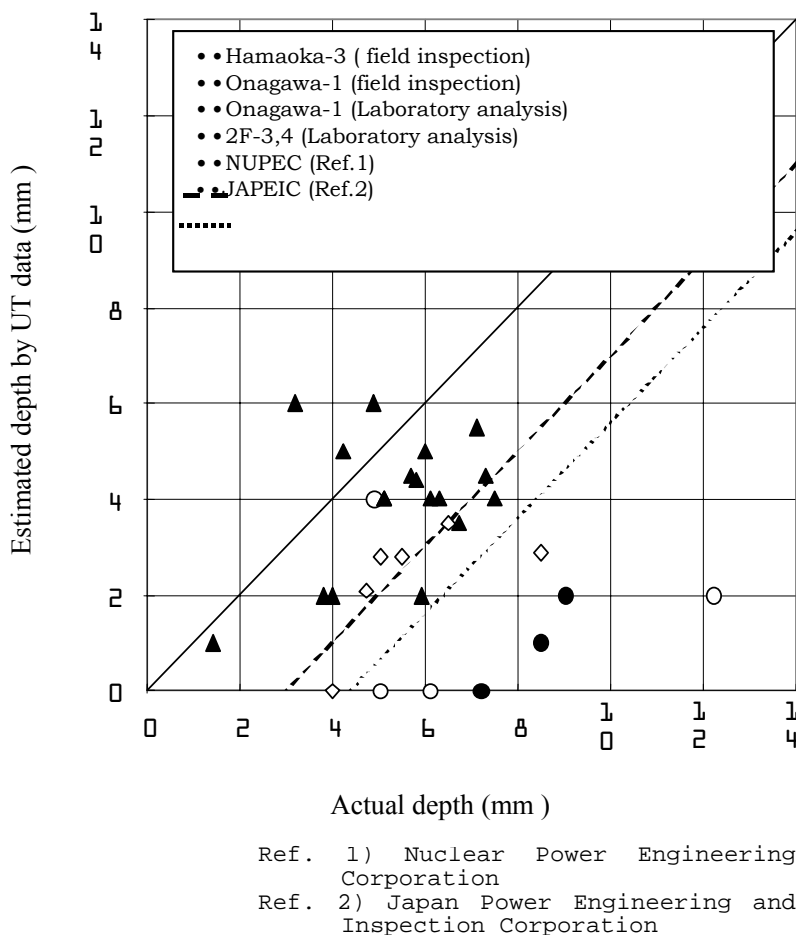


Fig. 10. Comparison between the estimated depth by UT data and the actual depth for PLR Cracks

#### 4. STRUCTURAL INTEGRITY EVALUATION FOR SHROUD

Shroud has two functions, support of reactor core and partition flow between core and annular region. To maintain its function, structural integrity under the load condition including earthquake is required, even if cracks exist. The integrity evaluation for cracked shroud is performed according to the philosophy of ASME sec. XI. Specifically, the evaluation was done as follows.

##### 4.1 Evaluation of a Cracked Shroud Ring

Since cracking was observed almost all around shroud ring, it was assumed that a circumferential crack of uniform depth would propagate uniformly in the radial direction. The crack was conservatively assumed to exist even in areas where cracking was not apparent. The average depth of the crack was measured by an ultrasonic inspection. The crack propagation in five years was then predicted by the following procedure:

- (1) Establish the initial crack configuration (depth).
- (2) Calculate the weld residual stress distribution by FEM in the crack propagation area.
- (3) Calculate stress intensity factor  $K_I$  from the crack depth and the residual stress distribution.
- (4) Use the SCC crack growth rate diagram from the experimental data to determine the crack growth rate for the calculated  $K$  value and then add the propagation to the initial crack depth.

By repeating calculations (3) and (4), the crack propagation in 5 years can be estimated. A limit load analysis to evaluate the structural integrity can then be performed.

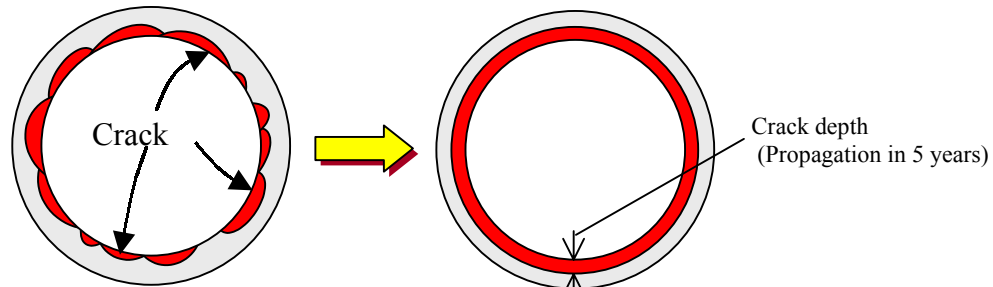


Fig. 11. Model for a Cracked Shroud Ring

##### 4.2 Evaluation of a Cracked Shroud Shell

In the shroud shell, a single crack has arisen and spread two-dimensionally on the surface. Since horizontal cracking is deleterious to shroud integrity, the spread crack is projected horizontally and regarded to be horizontal and straight. Although no through-wall cracking was found, all cracks are conservatively assumed to have penetrated. When the shroud shell has two or more cracks, even if these are not present at the same height, they are assumed to exist in the same level. To estimate the crack propagation in 5 years, the cracks are considered circumferentially with maximum SCC crack growth rate of low carbon SS. These grown cracks are gathered finally. A limit load analysis to evaluate the structural integrity can then be performed.

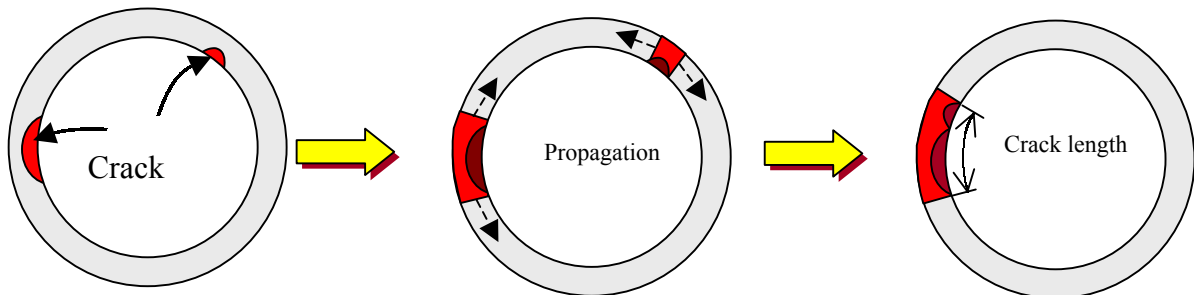
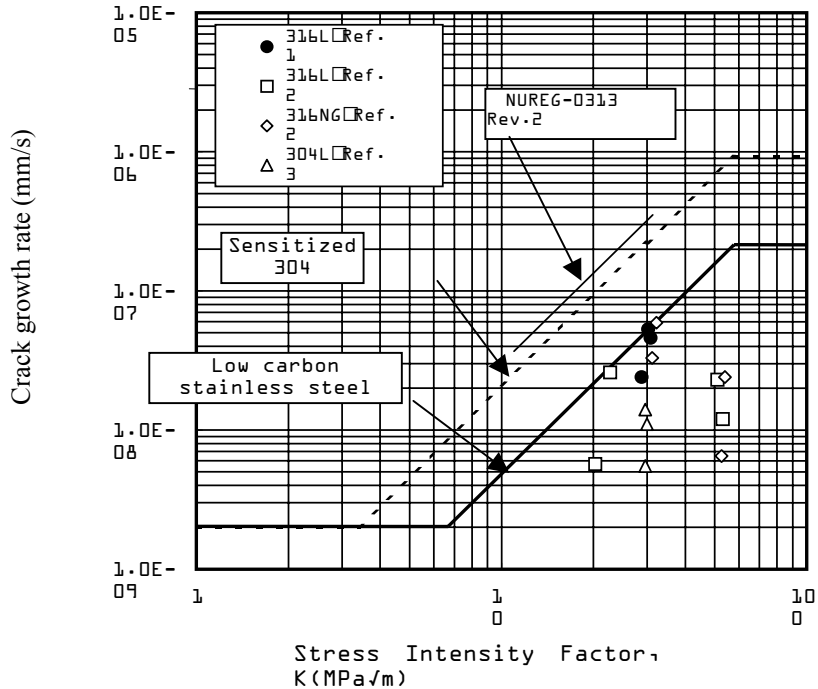


Fig. 12. Model for a Cracked Shroud Shell



### 4.3 SCC Crack Growth Rate

The crack growth rate diagram shown in Fig. 13, which represents the upper bound of the data obtained in the experiment on low-carbon SS, was used for estimating the crack propagation rate.



Ref.1) Thermal and Nuclear Engineering Society, "Guideline for inspection and evaluation of BWR reactor internals [core shroud]," JBWR-VIP-04, Nov 2001.

Ref.2) S. Namatame et al, "SCC crack growth rate diagram for austenite stainless in a simulated BWR environment," JSME symposium paper, 2933, pp.441-442, Sep 2002.

Ref.3 • in-house data, Sep 2000.

Fig. 13. SCC crack growth rate diagram for low-carbon stainless steel

### 4.4 Evaluation by fracture mechanics

Even if the stainless steel reactor internals in LWR are irradiated by neutrons, it is known that no extreme embrittlement occurs. However, austenitic stainless steels as type 316L and 304L begin to decrease in ductility when the neutron fluence exceeds  $3 \times 10^{24} \text{ n/m}^2$ . An evaluation by fracture mechanics was therefore taken into consideration near the core region welding lines (H4 and H3). Stress intensity  $K_I$  was calculated for the longest crack and compared with allowable value  $K_{IC}$ .

### 4.5 Results of the Structural Integrity Evaluation

Structural integrity evaluations were carried out for the cracked shrouds of 1F-4, 2F-3, 2F-4 and KK-1, -2 and

-3. A large safety margin was confirmed in the structural integrity of these shrouds at the present time and five years later. An example of the evaluation of the circumferential cracking in KK-2 is shown below.

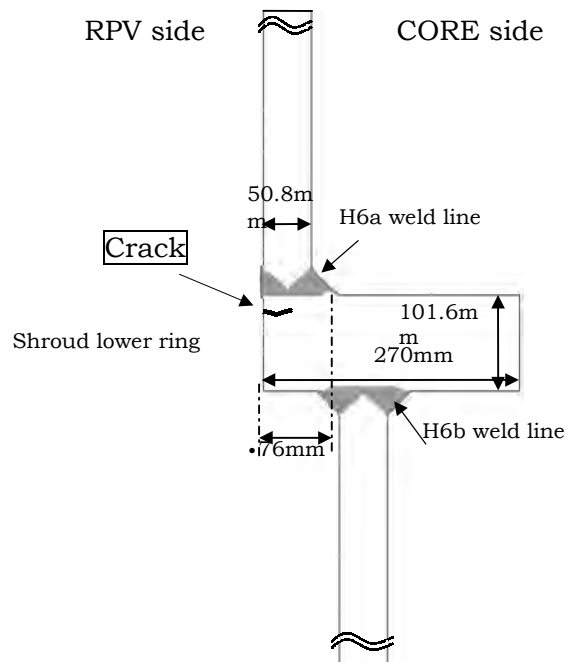


Fig. 14. Cracking in the Shroud Lower Ring of KK-2

Table 3. Structural integrity evaluation ( KK-2 lower ring )

Initial area (mm <sup>2</sup> )	Residual area except the crack at present time (mm <sup>2</sup> )	Residual area except the crack 5 years later (mm <sup>2</sup> )	Required area (mm <sup>2</sup> )
<b>8.3 x 10<sup>5</sup> (100%)</b>	<b>6.6 x 10<sup>5</sup> (79%)</b>	<b>5.1 x 10<sup>5</sup> (61%)</b>	<b>1.4 x 10<sup>5</sup> (17%)</b>

## 5. CONCLUSION

A large number of SCC cracks have been found in the core shrouds and PLR piping fabricated from low-carbon SS like type 316L in several Japanese BWRs. An investigation of this cracking, including a boat-sample analysis, was conducted to elucidate that the crack was initiated as mainly TGSCC from the surface hardened by cold working like machining or grinding during manufacture and propagated as IGSGG without any sensitization. An evaluation was performed of the structural integrity of the cracked shroud under conservative assumptions, and was confirmed to be sufficient at the present time and 5 years later. However, significant errors in the crack depth measurement of PLR piping was apparent, requiring the removal of the cracks or local replacement of the piping.